



Published in final edited form as:

*Neuron*. 2014 June 18; 82(6): 1263–1270. doi:10.1016/j.neuron.2014.04.038.

## Norepinephrine controls astroglial responsiveness to local circuit activity

Martin Paukert<sup>1,4,5,\*</sup>, Amit Agarwal<sup>1,5</sup>, Jaepyeong Cha<sup>2</sup>, Van A. Doze<sup>3</sup>, Jin U. Kang<sup>2</sup>, and Dwight E. Bergles<sup>1,\*</sup>

<sup>1</sup>Solomon H. Snyder Department of Neuroscience Johns Hopkins University School of Medicine 725 N. Wolfe St., WBSB 1001 Baltimore, MD 21205 USA

<sup>2</sup>Department of Electrical and Computer Engineering Johns Hopkins University 3400 N. Charles St. Baltimore, MD 21218 USA

<sup>3</sup>Department of Basic Sciences School of Medicine and Health Sciences University of North Dakota 501 N. Columbia Rd. Stop 9061 Grand Forks, ND 58202 USA

### SUMMARY

Astrocytes perform crucial supportive functions, including neurotransmitter clearance, ion buffering and metabolite delivery. They can also influence blood flow and neuronal activity by releasing gliotransmitters in response to intracellular  $Ca^{2+}$  transients. However, little is known about how astrocytes are engaged during different behaviors *in vivo*. Here we demonstrate that norepinephrine primes astrocytes to detect changes in cortical network activity. We show in mice that locomotion triggers simultaneous activation of astrocyte networks in multiple brain regions. This global stimulation of astrocytes was inhibited by alpha-adrenoceptor antagonists and abolished by depletion of norepinephrine from the brain. Although astrocytes in visual cortex of awake mice were rarely engaged when neurons were activated by light stimulation alone, pairing norepinephrine release with light stimulation markedly enhanced astrocyte  $Ca^{2+}$  signaling. Our findings indicate that norepinephrine shifts the gain of astrocyte networks according to behavioral state, enabling astrocytes to respond to local changes in neuronal activity.

---

© 2014 Elsevier Inc. All rights reserved.

\*Correspondence: paukertm@uthscsa.edu or dbergles@jhmi.edu.

<sup>4</sup>present address: Department of Physiology University of Texas Health Science Center at San Antonio 8403 Floyd Curl Drive, STRF 208.2 San Antonio, TX 78229 USA

<sup>5</sup>Co-first authors

Additional information about the procedures used in this study is described in the Supplemental Experimental Procedures.

SUPPLEMENTAL INFORMATION Supplemental Information includes Supplemental Experimental Procedures, four figures and 3 movies and can be found with this article online.

**Author Contributions.** M.P. and D.E.B. conceived of the project, designed the experiments and wrote the manuscript with help from the other authors. M.P. conducted experiments, developed software and analyzed data. A.A. generated and characterized the *R26-lsl-GCaMP3* mice, J.C. and J.K. developed the dual fiber imaging probe and assisted with fiber optic imaging, and V.A.D. provided assistance with adrenergic receptor pharmacology.

**Publisher's Disclaimer:** This is a PDF file of an unedited manuscript that has been accepted for publication. As a service to our customers we are providing this early version of the manuscript. The manuscript will undergo copyediting, typesetting, and review of the resulting proof before it is published in its final citable form. Please note that during the production process errors may be discovered which could affect the content, and all legal disclaimers that apply to the journal pertain.

## INTRODUCTION

Astrocytes are an essential component of neural circuits *in vivo*. They form highly interconnected networks, in which individuals occupy distinct domains that are extensively coupled through gap junctions. Each cell extends highly ramified processes that ensheath synapses, make contact with nodes of Ranvier and form endfeet specializations on blood vessels, placing these cells in an ideal position to both control the extracellular milieu and influence neuronal activity. Indeed, astrocytes have been shown to participate in diverse functions, including neurotransmitter clearance, ion homeostasis (Djukic et al., 2007), hemodynamic control (Mulligan and MacVicar, 2004), and synaptic plasticity (Min and Nevian, 2012). However, there is still uncertainty about how astrocyte networks are controlled *in vivo* and when they engage in these distinct behaviors.

Astrocytes express an extensive complement of Gq-coupled neurotransmitter receptors that liberate  $\text{Ca}^{2+}$  from intracellular stores, providing a means to adjust their behavior in response to changes in neural activity.  $\text{Ca}^{2+}$  signaling in astrocytes has been linked to diverse phenomena, including changes in blood vessel diameter (Attwell et al., 2010; Mulligan and MacVicar, 2004) and synaptic plasticity (Di Castro et al., 2011; Min and Nevian, 2012; Jourdain et al., 2007), suggesting that the impact of astrocytes on various aspects of brain physiology is controlled by these metabotropic receptors. Nevertheless, the role of  $\text{Ca}^{2+}$  signaling in astrocytes *in vivo* remains uncertain, and mice that lack IP3R2  $\text{Ca}^{2+}$  release channels that are responsible for receptor evoked  $\text{Ca}^{2+}$  transients are overtly normal (Petraevicz et al., 2008). Our lack of understanding about the interaction of astrocytes with neural circuits reflects our limited knowledge about the behavioral contexts in which astrocyte networks are activated. Despite evidence that astrocytes are responsive to multiple neurotransmitters, the pathways used to activate astrocytes *in vivo* and the patterns of activity that they exhibit during different behaviors remain to be defined.

*In vivo* two photon imaging using  $\text{Ca}^{2+}$  sensitive dyes has revealed that astrocyte network activity can be enhanced by local glutamatergic signaling (Nimmerjahn et al., 2009; Schummers et al., 2008) or by stimulation of long-range cholinergic (Takata et al., 2011; Chen et al., 2012) or noradrenergic (Bekar et al., 2008; Ding et al., 2013) neuromodulatory projections. How these local and global neuronal pathways interact to control the activity of astrocyte networks in awake, behaving animals has not been determined. Here we developed mice that express the genetically encoded  $\text{Ca}^{2+}$  indicator GCaMP3 in astrocytes and used *in vivo* two photon imaging to define the activity patterns of cortical and cerebellar astrocytes during locomotion. Our results indicate that the increase in arousal that accompanies locomotion promotes widespread activation of astrocyte networks in the cortex, and enhances their responsiveness to local changes in neuronal activity.

## RESULTS

### **$\text{Ca}^{2+}$ transients in Bergmann glia during locomotion depend on animal state of arousal**

To define the mechanisms that control astrocyte activity *in vivo*, we developed transgenic knock-in mice (*R26-lsl-GCaMP3*) in which the genetically encoded  $\text{Ca}^{2+}$  indicator GCaMP3 can be expressed in a cell specific manner (Figure S1). After breeding to *GLAST-CreER*

mice, tamoxifen administration induced GCaMP3 expression in  $35 \pm 2$  % of cortical astrocytes ( $n = 20$  mice) (Figure S1C) and 100% of Bergmann glia ( $n = 17$  mice), a distinct group of astroglial cells found in the cerebellar cortex (Figure 1A, Figure S1C), which could be visualized *in vivo* for weeks-to-months using two-photon imaging through a cranial window (Movie S1). Apart from neurons (dentate gyrus granule cells, olfactory bulb interneurons) derived from SVZ/SGZ progenitors that express GLAST, no neuronal expression was detected in these mice.

Locomotion has been shown to trigger a transient rise in intracellular  $\text{Ca}^{2+}$  in Bergmann glia (Nimmerjahn et al., 2009). This activity, visualized acutely with a  $\text{Ca}^{2+}$  indicator dye, extended over large areas of the cerebellum and required local activation of glutamate receptors. To define the mechanisms required to engage this glial network, we trained GCaMP3 expressing mice to walk on a treadmill and monitored locomotion-induced  $\text{Ca}^{2+}$  levels in Bergmann glia. In accordance with previous findings (Nimmerjahn et al., 2009), brief bouts of locomotion were often associated with widespread elevation of  $\text{Ca}^{2+}$  in Bergmann glia that persisted for many seconds after cessation of movement (Figure 1B, Movie S2). However, the magnitude of the Bergmann glia  $\text{Ca}^{2+}$  response was not correlated with locomotion speed ( $R = 0.0352$ ,  $p = 0.4365$ , 495 events from 4 mice), and locomotion often did not trigger activation of Bergmann glia (212 failures in 707 locomotion events). As comparable bouts of locomotion should produce similar activity in glutamatergic afferents, these results suggest that other signaling pathways are involved in recruitment of these glial cells. Indeed, Bergmann glia often exhibited widespread activity in the absence of locomotion (Figure 1D, E) (83 events, 4 mice).

To provide an independent measure of motor activity in these mice, we monitored muscle contraction during imaging trials. Post hoc analysis of electromyogram (EMG) recordings revealed that “spontaneous”  $\text{Ca}^{2+}$  transients that occurred in the absence of locomotion were often associated with an increase in EMG power (73/83 events, 3 mice), suggestive of startle behavior. This observation raised the possibility that activity in Bergmann glia may correspond to an increase in arousal. To facilitate pharmacological analysis of locomotion-induced Bergmann glial  $\text{Ca}^{2+}$  responses, we standardized their motor activity by subjecting mice to brief periods (5 s) of forced locomotion. Strikingly, enforced locomotion consistently evoked large  $\text{Ca}^{2+}$  transients throughout the Bergmann glia network (Figure 2A).  $\text{Ca}^{2+}$  transients induced by enforced locomotion had a similar time course to events that occurred during voluntary locomotion (enforced: half-maximum width,  $8.30 \pm 0.60$  s,  $n = 159$  events; voluntary:  $8.26 \pm 1.24$  s,  $n = 13$  events, 5 mice,  $p = 0.975$ ) (Figure 2B) and enforced events that immediately followed voluntary events were depressed by  $47 \pm 5$  % ( $n = 11$  events, 7 mice,  $p < 0.001$ ) (Figure 2C), suggesting that similar pathways are activated during both voluntary and enforced locomotion.

### Norepinephrine induces $\text{Ca}^{2+}$ elevations in Bergmann glia during locomotion

We assessed whether antagonists of different neuromodulatory receptors attenuated Bergmann glia  $\text{Ca}^{2+}$  changes induced by locomotion. Although Bergmann glia responses were not affected by peripheral administration of CNS accessible antagonists of serotonergic, muscarinic, metabotropic glutamate, or cannabinoid receptors, administration

of trazodone, a broad spectrum inhibitor of adrenergic, serotonergic and histaminergic receptors (Cusack et al., 1994), dramatically reduced locomotion-induced  $\text{Ca}^{2+}$  transients in these cells without altering intensity of their motor response (EMGs) (Figure 2D-F). Increases in arousal are often associated with the release of norepinephrine (Foote et al., 1980), raising the possibility that the trazodone-induced block of  $\text{Ca}^{2+}$  signaling in Bergmann glia is due to an inhibition of the noradrenergic signaling. Indeed, chemical depletion of norepinephrine with the neurotoxin DSP4 (Jonsson et al., 1981) abolished Bergmann glia  $\text{Ca}^{2+}$  transients induced by either voluntary and enforced locomotion (Figure S2), indicating that norepinephrine plays a key role in activating these astroglial cells during this behavior. The histaminergic H1 receptor antagonist diphenhydramine (DPH) also partially inhibited Bergmann glia responses, possibly due to its antagonism at  $\alpha$ 1-adrenoceptors (Kester et al., 2003). To define the receptor subtypes responsible, we locally applied selective adrenoceptor antagonists to the cerebellar surface between imaging sessions. Locomotion-induced  $\text{Ca}^{2+}$  transients were strongly inhibited by the  $\alpha$ 1-adrenergic receptor antagonist terazosin, but not by the  $\beta$ -adrenoceptor antagonist metoprolol (Figure 2G). In contrast, AMPA and NMDA receptor antagonists attenuated, but did not block this activity, suggesting that local glutamatergic and noradrenergic signaling act synergistically in the cerebellar cortex to promote Bergmann glia activity.

### **Locomotion-induced norepinephrine release activates astrocytes in visual cortex**

Noradrenergic neurons in the brainstem nucleus locus coeruleus (LC) extend axon collaterals diffusely throughout the brain, providing the means to exert control over brain activity states (Steindler, 1981). To determine if locomotion-induced engagement of the noradrenergic system results in global activation of astrocytes throughout the brain, we monitored astrocyte  $\text{Ca}^{2+}$  levels in primary visual cortex (V1) during locomotion (Figure 3A-C). Remarkably, in complete darkness, enforced locomotion reliably elicited  $\text{Ca}^{2+}$  transients in V1 astrocytes that had a similar time course to Bergmann glia responses in the cerebellum (Figure 3D, E, Movie S3). Locomotion-induced astrocyte activity in V1 was similarly blocked by trazodone and abolished by depletion of norepinephrine with DSP4 (Figure S3). To assess the relative timing and spatial extent of changes in astrocyte activity, we developed a dual fiber optic imaging system to monitor GCaMP3 fluorescence simultaneously in different brain regions (Figure 3F). When fiber optic probes were positioned over cranial windows implanted above the visual cortex (V1) and cerebellum (lobulus simplex), coincident  $\text{Ca}^{2+}$  elevations were detected in both astrocytes and Bergmann glia in response to voluntary and enforced locomotion (Figure 3G). The magnitude of  $\text{Ca}^{2+}$  changes in these two regions co-varied (correlation coefficient = 0.756,  $p < 0.001$ ;  $n = 348$  events from 6 mice), suggesting that amplitude fluctuations arise primarily from different levels of activity in noradrenergic neurons. Although events in these regions began at the same time (cerebellum onset delay =  $1.93 \pm 0.13$  s; V1 onset delay =  $1.91 \pm 0.10$  s, 348 events from 6 mice,  $p = 0.8982$ ), consistent with the minimal delay predicted to arise solely from differences in axonal length (~40 ms, assuming a conduction velocity of 0.5 m/s and an additional distance of 20 mm to V1),  $\text{Ca}^{2+}$  transients in visual cortex reached their peak  $1.6 \pm 0.2$  s later than events in the cerebellum ( $p < 0.001$ ), raising the possibility that local circuit activity modifies the timing of astrocyte recruitment.

## Norepinephrine enhances the sensitivity of astrocytes to local circuit activity

Locomotion induces release of norepinephrine in the visual cortex in complete darkness, providing a means to determine whether activation of this endogenous neuromodulatory input influences the response of astrocytes to local network activity. To assess the effects of norepinephrine, we monitored the behavior of groups of V1 astrocytes to locomotion, light stimulation alone, and locomotion paired with light stimulation. Enforced locomotion reliably elicited  $\text{Ca}^{2+}$  transients in V1 astrocytes, although the response of individual cells was variable, with some cells responding to each trial and others responding to only a subset of trials (Figure 4A, B). In contrast, light stimulation alone rarely activated V1 astrocytes, despite triggering large evoked potentials and inducing hemodynamic changes in this area (Figure S4A, B). Occasional coincident astrocyte activity that occurred in response to light stimulation was always associated with enhanced EMG power (Figure 4A), reflecting voluntary locomotion of the animals or possible startle behavior. Despite the weak activation of V1 astrocytes by visual input, pairing locomotion with light stimulation markedly enhanced astrocyte activity above that produced by locomotion alone, without altering motor output as measured by EMG (Figure 4A-D). Analysis of individual astrocytes revealed that light stimulation increased both the amplitude of  $\text{Ca}^{2+}$  transients in each cell and the proportion of cells that responded to each trial (Figure 4B, C). To assess whether the highly ramified processes of astrocytes, which are comprised of distinct microdomains (Grosche et al., 1999), exhibit  $\text{Ca}^{2+}$  transients with thresholds and kinetics distinct from those observed at the soma, we analyzed  $\text{Ca}^{2+}$  events in astrocyte processes and somata independently by masking individual astrocyte somata within the field; these non-somatic regions yielded signals from both the main processes and the highly ramified segments within the neuropil. Although it is possible that some microdomain activity may go undetected using our imaging method, astrocyte processes responded very similarly to their somata (Figure S4C-H), suggesting that alpha1 adrenoceptors are widely distributed in astrocyte membranes.

## DISCUSSION

These findings indicate that astrocytes throughout the brain are activated by norepinephrine during periods of heightened vigilance, and that this modulation plays a critical role in enabling these glial cells to respond to local network activity. Unlike fast excitatory and inhibitory neurotransmitters, where transmission occurs at synapses defined by directly apposed pre- and postsynaptic elements, norepinephrine is released from axonal varicosities into the surrounding neuropil, a “volume transmission” that enables multiple targets in the surrounding area to be affected. Astroglia appear to be a direct target of the noradrenergic system, as gene expression profiling indicates that they express a variety of Gq-coupled alpha adrenergic receptors (Cahoy et al., 2008), exogenous norepinephrine triggers a rise in  $\text{Ca}^{2+}$  in cultured astrocytes (Salm and McCarthy, 1990) as well as astrocytes and Bergmann glia in acute brain slices when neuronal activity is blocked (Duffy and MacVicar, 1995; Shao and McCarthy, 1997), and aversive stimuli or direct electrical stimulation of the locus coeruleus induces  $\text{Ca}^{2+}$  transients in astrocytes in the somatosensory cortex (Bekar et al., 2008; Ding et al., 2013). The mechanisms that enhance the responsiveness of astrocytes to local increases in neuronal activity are unknown, but may involve intracellular changes in

signaling intermediates that enhance the ability of other Gq-coupled metabotropic receptors to induce  $\text{Ca}^{2+}$  release from intracellular stores (Ryzhov et al., 2006). It is also possible that synergy occurs by enhancing the release of norepinephrine in V1, leading to larger, more prolonged  $\text{Ca}^{2+}$  transients in astrocytes. This effect could be initiated locally in the cortex, or by enhancing the activity of these neurons at the level of the LC. Direct assessment of the activity of noradrenergic projections to V1 during this behavior would help to define whether their activity is modulated in this form of plasticity.

### Reduced responsiveness of astrocyte networks in unanesthetized mice

The close association of astrocytes with synapses allows detection of neuronal activity and the potential for feedback modulation (Parpura et al., 1994; Di Castro et al., 2011; Jourdain et al., 2007; Saab et al., 2012). Thus, it was unexpected that exposure to strong visual stimulation alone failed to engage astrocyte networks in V1, particularly given previous studies demonstrating robust activation of V1 astrocytes with light in anesthetized mice (Chen et al., 2012). However, anaesthesia has been shown to dramatically expand active regions in mouse V1 and prolong responses to visual stimulation (Haider et al., 2013), which may lower the threshold for astrocyte activation. Moreover, astrocytes have been implicated in the regulation of sleep-wake cycles (Halassa et al., 2009) and their functional state differs considerably between sleep/anaesthesia and wakefulness (Xie et al., 2013). It has also been reported that astrocyte  $\text{Ca}^{2+}$  signaling *in vivo* is inhibited by various anesthetics (Nimmerjahn et al., 2009; Thrane et al., 2012), raising concern that the depth of anesthesia and type of anesthetic can dramatically alter their responsiveness. Together, these findings highlight the importance of defining astrocyte activity in awake animals during different behavioral states.

### Norepinephrine enhances the gain of both astrocyte and neuronal networks

These studies indicate that astrocyte networks have a high threshold for activation in periods of quiescence, and suggest that recruitment of the noradrenergic system is required to enhance the gain of these networks to enable local interactions between astrocytes and neurons in circuits involved in processing sensory information. The activation of astrocytes in V1 by norepinephrine during locomotion parallels recent *in vivo* electrophysiological studies indicating that locomotion triggers norepinephrine-dependent depolarization of neurons in V1 (Polack et al., 2013). In contrast to neuronal activation, which began within 50 ms of locomotion onset,  $\text{Ca}^{2+}$  transients in astrocytes began more than a second later ( $1.4 \pm 0.1$  s,  $n = 106$  events from 13 mice), presumably reflecting the additional biochemical steps required to release  $\text{Ca}^{2+}$  from intracellular stores. These results suggest that astrocyte  $\text{Ca}^{2+}$  transients are unlikely to be causal for the initial depolarization of cortical neurons, for example, by stimulating the release of gliotransmitters; however,  $\text{Ca}^{2+}$  is not the only signaling intermediate produced by activation of alpha adrenoceptors and astrocytes may express adrenoceptors coupled to other G-proteins (e.g. Gi) (Cahoy et al., 2008) that could trigger responses on a timescale co-incident with neuronal depolarization. The ability of astroglia to detect the coincidence of arousal and local network activity may allow these cells to contribute to sensory-specific attentional shifts (Cohen and Maunsell, 2011), promoted by the slow onset and prolonged nature of their  $\text{Ca}^{2+}$  responses. Future analysis of



mice in which alpha adrenoceptors have been selectively removed from astrocytes will help to define their role in noradrenergic modulation of cortical networks and arousal states.

Astrocytes are well positioned to amplify the effects of diffuse neuromodulatory projections; their highly ramified processes not only increase the probability of interaction with low concentrations of neurotransmitters, but also shield neurons by increasing the diffusional distance from varicosities to neuronal membranes. Although the exact complement of neurotransmitter receptors expressed by astrocytes in different brain regions has not been defined, cortical astrocytes have also been shown to respond to glutamate, ATP and acetylcholine (Verkhratsky and Kettenmann, 1996; Takata et al., 2011). The ability to stably express  $Ca^{2+}$  indicators selectively in astrocytes *in vivo* using conditional GCaMP3 mice will help define the behavioral contexts in which these different receptors become activated and reveal how they influence interactions between neurons and astrocytes in distinct neural circuits.

## EXPERIMENTAL PROCEDURES

### Animals

Cre recombinase-conditional GCaMP3 mice were generated using a knock-in strategy into the ROSA26 locus and crossed to *GLAST-CreER* mice to enable GCaMP3 expression in astrocytes and Bergmann glia. Cranial windows were implanted above the cerebellum or V1.

### *In vivo* two-photon imaging

Fluorescence images were collected using a Movable Objective Microscope (MOM) (Sutter Instruments) with a 20x, 1.0 NA objective (Zeiss). Image acquisition rate was 2 frames/s.

### Dual optic fiber bundle imaging

For simultaneous imaging of astroglial  $Ca^{2+}$  changes in cerebellum and visual cortex, cranial windows were implanted and two multicore optical fibers aligned above these regions. The light path is illustrated in Figure 3F. No optical cross-talk between fiber bundles was detected: The objective lens pairs had a diameter of 2.4 mm and a working distance of 0.88 mm.

### Locomotion behavioral paradigm

Mice were placed on a custom designed linear treadmill and their heads immobilized. The treadmill was either freely movable or placed under motor control and the motion of the treadmill belt was monitored with an optical encoder.

### Electromyography

Body surface potentials were recorded as the voltage difference between two silver wires placed subcutaneously at the right shoulder and left hip.

## Visual stimulation

A UV-LED with a Lambertian emission profile was used as a light source at a distance of 40 mm, centered between the eyes to achieve uniform light exposure.

## Data analysis

Data were processed and analyzed in MATLAB.  $F/F$  fluorescence intensity traces represent  $(F - F_{\text{median}}) / F_{\text{median}}$  with  $F$  representing mean fluorescence value of all pixels within a region of interest (ROI) of one image frame and  $F_{\text{median}}$  representing median  $F$  of all image frames.

## Statistical analysis

Figures 1E and 3H: analysis of co-variance for correlation within subjects; Figures 1B and C, 4D (right), difference in onset of response in Figure 3F-H, Figures S2 and S3, one-tailed paired  $t$  test; Figures 1F and G, 4C and D (left) one-way ANOVA followed by Bonferroni post-hoc test; text, difference in peak of response in Figure 3F-H, one-sample  $t$  test.

## Supplementary Material

Refer to Web version on PubMed Central for supplementary material.

## Acknowledgments

We thank L. Looger for providing the GCaMP3 construct, J. Nathans for providing *GLAST-CreER* mice and assistance with Rosa26 targeting, M. Fukaya for providing antibodies, Terry Shelley for his machining expertise, and Naqing Ye for assistance with animal colony maintenance. This work was supported by grants from the NIAAA, AA022239 to M.P., from the NIMH (Conte Center for Neuroscience, MH084020) and the Brain Science Institute at Johns Hopkins to D.E.B. A.A. was supported by a postdoctoral fellowship from the National Multiple Sclerosis Society.

## References

- Attwell D, Buchan AM, Charpak S, Lauritzen M, MacVicar BA, Newman EA. Glial and neuronal control of brain blood flow. *Nature*. 2010; 468:232–243. [PubMed: 21068832]
- Bekar LK, He W, Nedergaard M. Locus coeruleus alpha-adrenergic-mediated activation of cortical astrocytes in vivo. *Cereb. Cortex*. 2008; 18:2789–2795. [PubMed: 18372288]
- Cahoy JD, Emery B, Kaushal A, Foo LC, Zamanian JL, Christopherson KS, Xing Y, Lubischer JL, Krieg PA, Krupenko SA, et al. A transcriptome database for astrocytes, neurons, and oligodendrocytes: a new resource for understanding brain development and function. *J. Neurosci*. 2008; 28:264–278. [PubMed: 18171944]
- Di Castro MA, Chuquet J, Liaudet N, Bhaukaurally K, Santello M, Bouvier D, Tiret P, Volterra A. Local Ca<sup>2+</sup> detection and modulation of synaptic release by astrocytes. *Nat. Neurosci*. 2011; 14:1276–1284. [PubMed: 21909085]
- Chen N, Sugihara H, Sharma J, Perea G, Petracicz J, Le C, Sur M. Nucleus basalis-enabled stimulus-specific plasticity in the visual cortex is mediated by astrocytes. *Proc. Natl. Acad. Sci. U. S. A*. 2012; 109:E2832–41. [PubMed: 23012414]
- Cohen MR, Maunsell JHR. Using neuronal populations to study the mechanisms underlying spatial and feature attention. *Neuron*. 2011; 70:1192–1204. [PubMed: 21689604]
- Cusack B, Nelson A, Richelson E. Binding of antidepressants to human brain receptors: focus on newer generation compounds. *Psychopharmacology (Berl)*. 1994; 114:559–565. [PubMed: 7855217]



- Ding F, O'Donnell J, Thrane AS, Zeppenfeld D, Kang H, Xie L, Wang F, Nedergaard M.  $\alpha$ 1-Adrenergic receptors mediate coordinated Ca(2+) signaling of cortical astrocytes in awake, behaving mice. *Cell Calcium*. 2013; 54:387–394. [PubMed: 24138901]
- Djukic B, Casper KB, Philpot BD, Chin L-S, McCarthy KD. Conditional knockout of Kir4.1 leads to glial membrane depolarization, inhibition of potassium and glutamate uptake, and enhanced short-term synaptic potentiation. *J. Neurosci*. 2007; 27:11354–11365. [PubMed: 17942730]
- Duffy S, MacVicar BA. Adrenergic calcium signaling in astrocyte networks within the hippocampal slice. *J. Neurosci*. 1995; 15:5535–5550. [PubMed: 7643199]
- Foote SL, Aston-Jones G, Bloom FE. Impulse activity of locus coeruleus neurons in awake rats and monkeys is a function of sensory stimulation and arousal. *Proc. Natl. Acad. Sci. U. S. A.* 1980; 77:3033–3037. [PubMed: 6771765]
- Grosche J, Matyash V, Möller T, Verkhratsky A, Reichenbach A, Kettenmann H. Microdomains for neuron-glia interaction: parallel fiber signaling to Bergmann glial cells. *Nat. Neurosci*. 1999; 2:139–143. [PubMed: 10195197]
- Haider B, Häusser M, Carandini M. Inhibition dominates sensory responses in the awake cortex. *Nature*. 2013; 493:97–100. [PubMed: 23172139]
- Halassa MM, Florian C, Fellin T, Munoz JR, Lee S-Y, Abel T, Haydon PG, Frank MG. Astrocytic modulation of sleep homeostasis and cognitive consequences of sleep loss. *Neuron*. 2009; 61:213–219. [PubMed: 19186164]
- Jonsson G, Hallman H, Ponzio F, Ross S. DSP4 (N-(2-chloroethyl)-N-ethyl-2-bromobenzylamine)--a useful denervation tool for central and peripheral noradrenaline neurons. *Eur. J. Pharmacol*. 1981; 72:173–188. [PubMed: 6265244]
- Jourdain P, Bergersen LH, Bhaukaurally K, Bezzi P, Santello M, Domercq M, Matute C, Tonello F, Gundersen V, Volterra A. Glutamate exocytosis from astrocytes controls synaptic strength. *Nat. Neurosci*. 2007; 10:331–339. [PubMed: 17310248]
- Kester RR, Mooppan UM, Gousse AE, Alver JE, Gintautas J, Gulmi FA, Abadir AR, Kim H. Pharmacological characterization of isolated human prostate. *J. Urol*. 2003; 170:1032–1038. [PubMed: 12913765]
- Min R, Nevian T. Astrocyte signaling controls spike timing-dependent depression at neocortical synapses. *Nat. Neurosci*. 2012; 15:746–753. [PubMed: 22446881]
- Mulligan SJ, MacVicar BA. Calcium transients in astrocyte endfeet cause cerebrovascular constrictions. *Nature*. 2004; 431:195–199. [PubMed: 15356633]
- Nimmerjahn A, Mukamel EA, Schnitzer MJ. Motor behavior activates Bergmann glial networks. *Neuron*. 2009; 62:400–412. [PubMed: 19447095]
- Parpura V, Basarsky TA, Liu F, Jęftinija K, Jęftinija S, Haydon PG. Glutamate-mediated astrocyte-neuron signalling. *Nature*. 1994; 369:744–747. [PubMed: 7911978]
- Petravic J, Fiacco TA, McCarthy KD. Loss of IP3 receptor-dependent Ca<sup>2+</sup> increases in hippocampal astrocytes does not affect baseline CA1 pyramidal neuron synaptic activity. *J. Neurosci*. 2008; 28:4967–4973. [PubMed: 18463250]
- Polack P-O, Friedman J, Golshani P. Cellular mechanisms of brain state-dependent gain modulation in visual cortex. *Nat. Neurosci*. 2013; 16:1331–1339. [PubMed: 23872595]
- Pologruto TA, Sabatini BL, Svoboda K. ScanImage: flexible software for operating laser scanning microscopes. *Biomed. Eng. Online*. 2003; 2:13. [PubMed: 12801419]
- Ryzhov S, Goldstein AE, Biaggioni I, Feoktistov I. Cross-talk between G(s)- and G(q)-coupled pathways in regulation of interleukin-4 by A(2B) adenosine receptors in human mast cells. *Mol. Pharmacol*. 2006; 70:727–735. [PubMed: 16707627]
- Saab AS, Neumeyer A, Jahn HM, Cupido A, Šimek AAM, Boele H-J, Scheller A, Le Meur K, Götz M, Monyer H, et al. Bergmann glial AMPA receptors are required for fine motor coordination. *Science*. 2012; 337:749–753. [PubMed: 22767895]
- Salm AK, McCarthy KD. Norepinephrine-evoked calcium transients in cultured cerebral type 1 astroglia. *Glia*. 1990; 3:529–538. [PubMed: 2148555]
- Schummers J, Yu H, Sur M. Tuned responses of astrocytes and their influence on hemodynamic signals in the visual cortex. *Science*. 2008; 320:1638–1643. [PubMed: 18566287]

- Shao Y, McCarthy KD. Responses of Bergmann glia and granule neurons in situ to N-methyl-D-aspartate, norepinephrine, and high potassium. *J. Neurochem.* 1997; 68:2405–2411. [PubMed: 9166734]
- Steindler DA. Locus coeruleus neurons have axons that branch to the forebrain and cerebellum. *Brain Res.* 1981; 223:367–373. [PubMed: 6169404]
- Takata N, Mishima T, Hisatsune C, Nagai T, Ebisui E, Mikoshiba K, Hirase H. Astrocyte calcium signaling transforms cholinergic modulation to cortical plasticity in vivo. *J. Neurosci.* 2011; 31:18155–18165. [PubMed: 22159127]
- Thrane AS, Rangroo Thrane V, Zeppenfeld D, Lou N, Xu Q, Nagelhus EA, Nedergaard M. General anesthesia selectively disrupts astrocyte calcium signaling in the awake mouse cortex. *Proc. Natl. Acad. Sci. U. S. A.* 2012; 109:18974–18979. [PubMed: 23112168]
- Verkhatsky A, Kettenmann H. Calcium signalling in glial cells. *Trends Neurosci.* 1996; 19:346–352. [PubMed: 8843604]
- Xie L, Kang H, Xu Q, Chen MJ, Liao Y, Thiyagarajan M, O'Donnell J, Christensen DJ, Nicholson C, Iliff JJ, et al. Sleep drives metabolite clearance from the adult brain. *Science.* 2013; 342:373–377. [PubMed: 24136970]

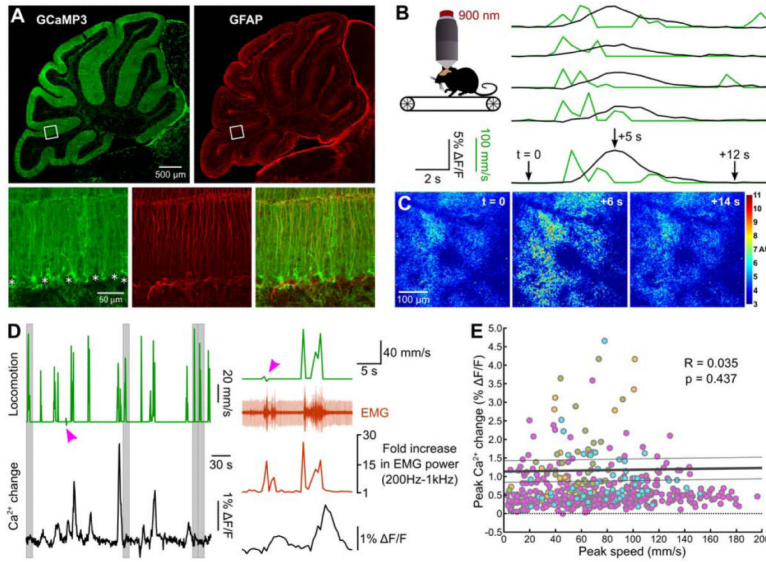


**Figure 1. Weak correlation between voluntary locomotion and Ca<sup>2+</sup> elevation in Bergmann glia**  
**A**, Cerebellar section from 5 week-old *GLAST-CreER;R26-lsl-GCaMP3* mouse immunostained for GCaMP3 and glial fibrillary acidic protein (GFAP). Boxed areas are shown at higher magnification below. Asterisks highlight Purkinje cell somata devoid of fluorescence. **B**, Left, schematic of imaging configuration. Right, five representative trials showing Bergmann glia Ca<sup>2+</sup> increase (GCaMP3 fluorescence, black traces) relative to mouse locomotion (optical encoder, green traces). **C**, Images of GCaMP3 fluorescence in Bergmann glial processes at times indicated by arrows in **B**. **D**, Left, continuous record of locomotion (green trace) and Bergmann glia Ca<sup>2+</sup> levels (GCaMP3 fluorescence). Grey bars highlight periods when locomotion was not associated with Bergmann glia Ca<sup>2+</sup> elevations. Arrowhead highlights a Bergmann glia Ca<sup>2+</sup> transient that was not associated with locomotion. Right, expanded portion of trial including electromyography (EMG) signal. Arrowhead indicates timing of Bergmann glia Ca<sup>2+</sup> elevation. **E**, Plot of locomotion speed and Bergmann glia Ca<sup>2+</sup> change (GCaMP3 fluorescence) for 707 locomotion periods from 4 mice. Colors represent trails from different individuals. Black lines represent mean ± SEM of 4 regression lines.

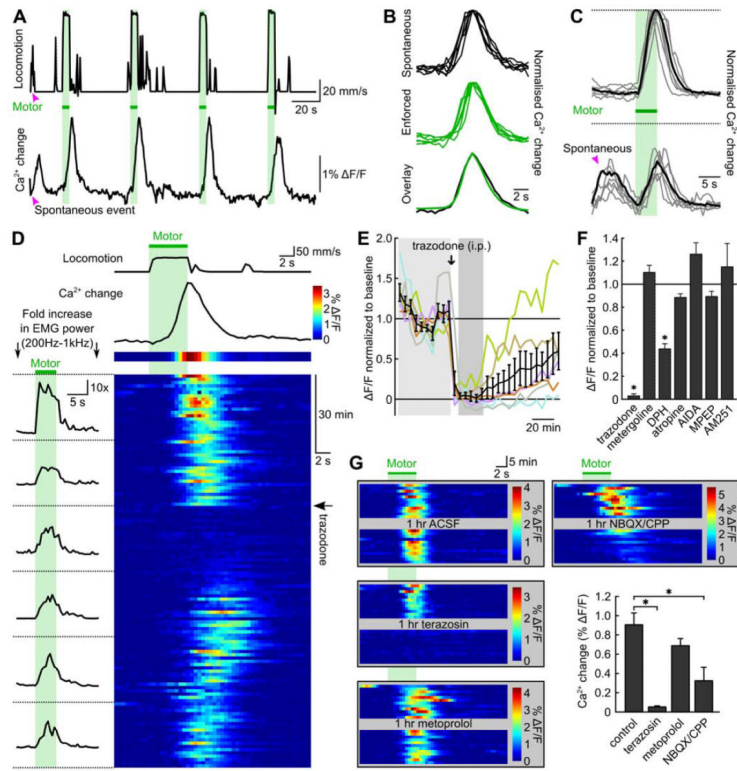


**Figure 2. Noradrenergic signaling is required for locomotion-induced activation of Bergmann glia**

**A**, Spontaneous (arrowhead) and enforced (green bars) locomotion and corresponding Bergmann glia  $Ca^{2+}$  levels (GCaMP3 fluorescence). **B**, Normalized Bergmann glia  $Ca^{2+}$  changes associated with spontaneous (6 of 13 events) and enforced locomotion (6 of 159 events) from experiment in **A**. **C**, Individual (gray traces) and average (black traces) Bergmann glia  $Ca^{2+}$  transients resulting from enforced locomotion with (lower traces) or without (upper traces) a preceding spontaneous event. **D**, Consecutive trials of enforced locomotion (green bar) pseudocolored according to magnitude of  $Ca^{2+}$  change. Arrow indicates time of trazodone injection (10 mg/kg i.p.). Left, average EMG power during 20 consecutive trials at right. **E**, Normalized amplitude of Bergmann glia  $Ca^{2+}$  elevations elicited by enforced locomotion. Each point is average of 4 consecutive trials normalized to baseline. Regions highlighted by light grey bar used to determine baseline and dark grey bar the maximal response to drug. Black symbols represent mean  $\pm$  SEM. **F**, Effect of neuromodulatory receptor antagonists on Bergmann glia  $Ca^{2+}$  response to enforced locomotion. Columns represent mean  $\pm$  SEM. Concentrations from left (mg/kg i.p.): 10, 10, 20, 20, 20, 20, 10. Number of experiments from left: 6, 5, 5, 5, 5, 4, 3. Asterisks indicate significant reduction relative to baseline in one-way ANOVA followed by Bonferroni post-hoc test. **G**, Bergmann glia  $Ca^{2+}$  transients in consecutive trials of enforced locomotion before and after local application of antagonists. Summary graph is mean  $\pm$  SEM. Concentrations ( $\mu$ M): 100 terazosin, 3 metoprolol, 300/200 NBQX/CPP. Number of experiments from left: 8, 5, 5, 5. Asterisks indicate significant difference in one-way ANOVA followed by Bonferroni post-hoc test.

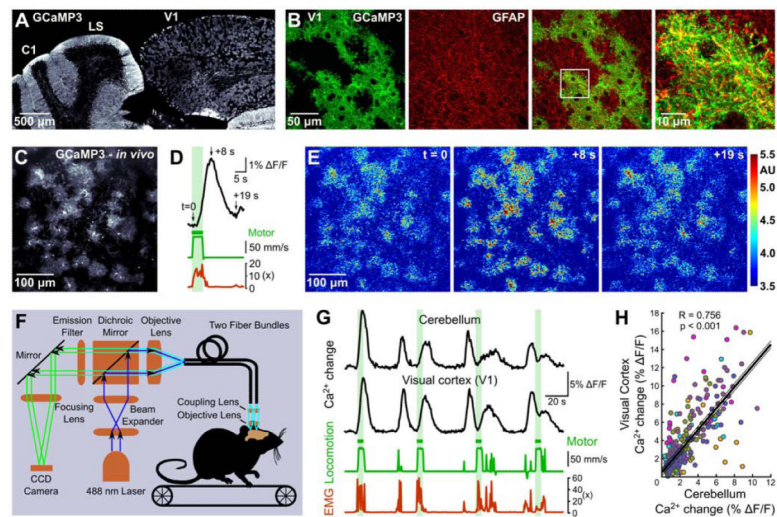


**Figure 3. Locomotion induces simultaneous activation of astroglia in different regions of the brain**

**A**, Parasagittal section of *GLAST-CreER;R26-lsl-GCaMP3* mouse (P57) immunostained for GCaMP3. crus1 (C1), lobulus simplex (LS), primary visual cortex (V1). **B**, Higher magnification image of GCaMP3 (green) and GFAP (red) in V1. **C**, *In vivo* image of V1, layer 1 (70  $\mu\text{m}$  below pial surface) cortical astrocytes expressing GCaMP3 in 3 month-old *GLAST-CreER;R26-lsl-GCaMP3* mouse. **D**, Mean change in cytosolic  $\text{Ca}^{2+}$  (GCaMP3) in V1 cortical astrocytes (black trace) induced by enforced locomotion (green trace). Green bar: period of enforced locomotion; green trace: locomotion; red trace fold increase in EMG activity. **E**, Images of GCaMP3 fluorescence in V1 astrocytes at times indicated in D. **F**, Schematic of dual fiber optic photometry configuration. **G**,  $\text{Ca}^{2+}$  changes in Bergmann glia and V1 astrocytes visualized simultaneously during enforced locomotion (green bars) and corresponding EMG activity. **H**, Co-variance between Bergmann glia and V1 astrocyte  $\text{Ca}^{2+}$  changes during spontaneous locomotion.  $n = 348$  spontaneous locomotion events from 6 mice. Black lines represent mean  $\pm$  SEM of 6 regression lines.



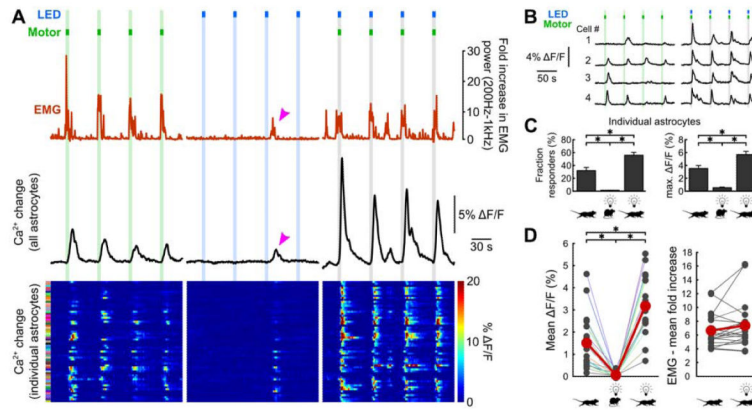


**Figure 4. Norepinephrine enhances the sensitivity of astrocytes to local circuit activity**  
**A**, V1 astrocyte  $Ca^{2+}$  responses to enforced locomotion (green bars), visual stimulation (blue bars) or simultaneous enforced locomotion and visual stimulation (gray bars). Red traces represent EMG activity, black traces represent mean  $Ca^{2+}$  change in all astrocytes. Lower panel represents  $Ca^{2+}$  changes in individual astrocytes pseudocolored according to amplitude. Arrowhead highlights  $Ca^{2+}$  elevation associated with spontaneous locomotion. **B**,  $Ca^{2+}$  transients in 4 representative cells during 4 consecutive trials of enforced locomotion (green bars) or simultaneous enforced locomotion and visual stimulation (grey bars). **C**, Left, average fraction of astrocytes responding with a mean  $Ca^{2+}$  elevation exceeding 1% F/F. Right, average maximum  $Ca^{2+}$  responses in individual astrocytes (16 - 20 trials). Bars represent mean  $\pm$  SEM;  $n = 20$  mice; asterisks indicate significant difference (one-way ANOVA with Bonferroni post-hoc test). **D**, Left, mean  $Ca^{2+}$  elevations in all astrocytes (16 - 20 trials). Colored lines connect data points from individual mice. Asterisks indicate significant difference (one-way ANOVA with Bonferroni post-hoc test). Right, change in EMG power during enforced locomotion or simultaneous enforced locomotion and visual stimulation. Each point represents average response in 16 - 20 trials. Red circles indicate mean of all trials.